

## NOTES

## Investigation of thermal contact resistance in injection molding using a hollow waveguide pyrometer and a two-thermocouple probe

A. Bendada,<sup>a)</sup> A. Derdouri, M. Lamontagne, and Y. Simard

National Research Council Canada, 75 De Mortagne, Boucherville, Quebec J4B 6Y4, Canada

(Received 2 June 2003; accepted 31 August 2003)

This Note describes an apparatus that characterizes the nature of thermal contact between polymer and mold through the different phases of a typical injection molding cycle. The key idea is the combination of the measurements provided by a hollow waveguide pyrometer and a two-thermocouple probe to determine the thermal contact resistance (TCR). The hollow waveguide pyrometer is used for the on-line monitoring of the temperature at the surface of the polymer stream, while the two-thermocouple probe is utilized to determine via an inverse heat conduction procedure the heat flux crossing the polymer-mold interface and the temperature at the cavity surface. The experimental results show that TCR between polymer and mold is not negligible and not constant with time. [DOI: 10.1063/1.1621063]

In injection molding, the characterization of the thermal contact between polymer and mold and the prediction of its evolution with pertinent process parameters are very difficult. The reason is its dependence on boundary conditions that cannot be measured reliably using conventional procedures such as thermocouples and heat flux transducers that may affect the heat transfer at the interface. In this Note, we describe a methodology that is based on the combination of two noninvasive sensors to characterize thermal contact resistance (TCR). This may be defined per surface unit as  $TCR = (T_{ps} - T_{ms})/\varphi$ , where  $T_{ps}$  is the polymer surface temperature,  $T_{ms}$  is the mold surface temperature, and  $\varphi$  is the heat flux density crossing the interface. To determine polymer surface temperature  $T_{ps}$ , we used a hollow waveguide pyrometer that has been already described in the scientific literature.<sup>1</sup> Mold surface temperature  $T_{ms}$  and heat flux density  $\varphi$  were indirectly obtained with the use of a specially designed two-thermocouple probe. Figure 1 shows an image of the probe. The latter was composed of two steel half-cylinders joined side by side. These were obtained by cutting longitudinally a cylinder that was 8 mm in diameter and 13 cm long. The shape and size of the cylinder tip planned to be in contact with the polymer stream were designed to fit commonly employed probe-housing cavities in injection molds. Two E-type fine-wire thermocouples 75  $\mu\text{m}$  in diameter were spot-welded inside the probe at two different locations (1 and 2 mm) from the probe tip. At the interface between the two half-cylinders, a narrow slot was longitudinally machined in one half-cylinder to contain the thermocouples wires. The shape and the location of the slot are represented with a diagram in Fig. 1. Two thermocouples rather than a single thermocouple were utilized because the additional informa-

tion could aid in more accurately estimating the surface conditions. To perform perfectly nonintrusive measurements, the two-thermocouple probe was manufactured with the same steel (P20 steel grade) as the mold material and the same roughness as the cavity surface. Two conditioning modules amplified the thermocouple signals to a data acquisition system and control unit. The latter devices were piloted with a computer via a general purpose interface bus card. A signal processing software was used for the visualization and the exploitation of the experimental results.

From temperature histories monitored with the two-thermocouple probe, a regularized sequential inverse method allowed the estimation of both heat flux  $\varphi$  crossing the polymer-mold interface and temperature at the cavity surface  $T_{ms}$ . This data processing was based on Beck's method that used a combination of the function specification method and the future time steps concept.<sup>2</sup>

The accuracy of the calculations produced with the inversion algorithm was numerically assessed against the exact

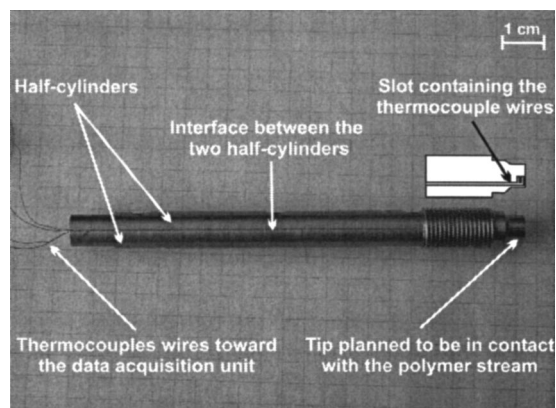


FIG. 1. Image of the two-thermocouple probe.

<sup>a)</sup>Electronic mail: abdelhakim.bendada@nrc.ca

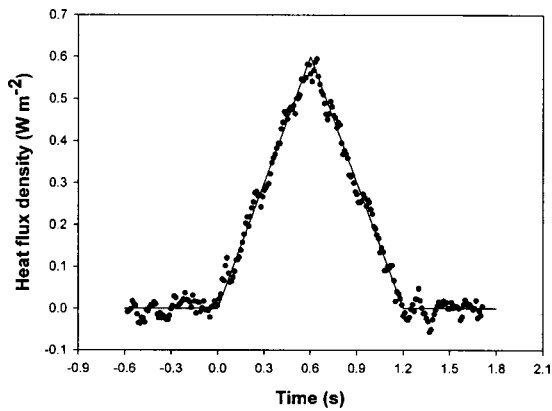


FIG. 2. Comparison of the calculated surface heat flux (●) using Beck's method and the true heat flux data (—).

solution of a heat flux that varied in time in a triangular fashion. The solid line curve in Fig. 2 illustrates the exact heat flux distribution. The test consisted in solving the heat transfer equation for the latter heat flux boundary condition and a uniform initial temperature field,  $T_0=0$ . Then, exact internal temperature distributions as a function of time at two different locations from the surface, namely 1 and 2 mm, were calculated. The solid line curve 1 in Fig. 3 is the exact temperature at 2 mm from the surface, while the solid line curve 2 is the exact temperature at 1 mm from the surface. To make the validation test more realistic, random errors generated numerically were added to the exact temperatures. The resulting simulated noisy temperatures are plotted in the same graph with triangle and square symbols, respectively. Subsequently, these two simulated temperatures were used as "experimental" inputs for the inverse heat conduction algorithm. The inversed heat flux and surface temperature are reported in Figs. 2 and 3, respectively, with the black circle curves. The results are quite stable and a good agreement between exact (solid line curves) and inversed data can be clearly observed.

After the theoretical validation of the inversion algorithm, experiments were carried out on a 250 ton Husky injection molding machine. The material used in the experiments was polypropylene. The nominal thickness of the in-

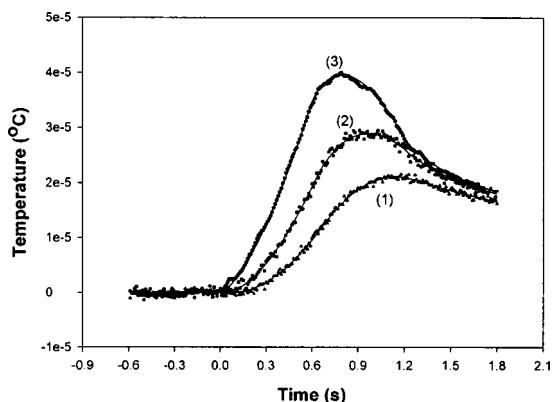


FIG. 3. Calculated temperature at the surface of the mold (●) using the internal simulated noisy temperatures at a distance of 1 (■) and 2 mm (▲), respectively from the mold surface. The solid line (—) curves are the true temperature data obtained by the solution of the forward problem.

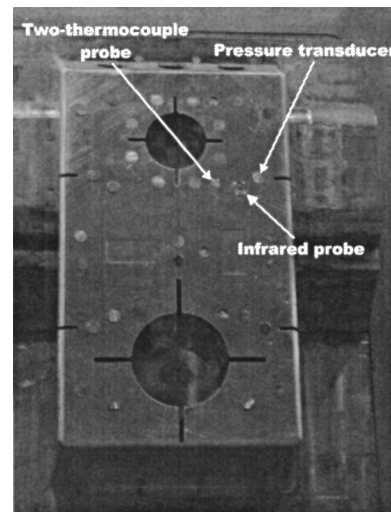


FIG. 4. Close up on the relative locations of the infrared probe, the pressure transducer, and the two-thermocouple probe incorporated into the mobile mold side of a Husky injection molding press.

jected part was 2.3 mm. Figure 4 is a close up image that shows the locations of three probes that were flush mounted with the cavity surface to monitor different process parameters. The hollow waveguide probe in the center was surrounded by the two-thermocouple probe on one side and a D.M.E SS-405C pressure transducer on the other side. Data acquisition for all sensors was performed at a frequency rate of 500 Hz so that rapid and sudden signal changes could be observed. The plastication conditions were set so that an injection temperature of 220 °C was achieved; the mold temperature was regulated at 25 °C, while the hydraulic pressure was set to 2.5 MPa. The injection rate was 11 cm/s, the packing time 1.75 s, and the holding time 3.5 s.

During the cooling, as the solidification progressed, the part begun to shrink through its thickness and an air gap was likely to be formed at the polymer mold interface. After a sizable gap was developed, the interface returned to the steel-air condition, and therefore, the pressure dropped back to its minimum level.<sup>1</sup> As soon as the relative pressure became equal to zero (at ~12 s), the heat transfer near the interface

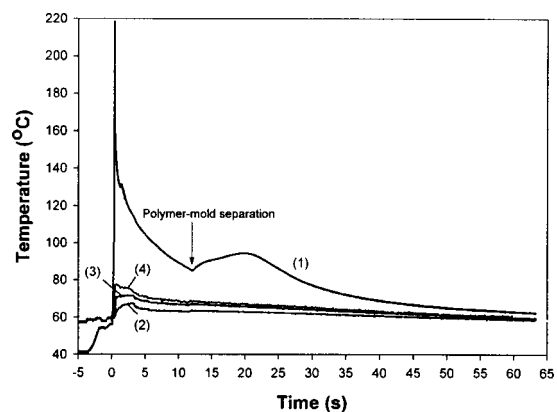


FIG. 5. Temperature traces in the mold and at the surface of the polymer stream: (1) temperature at the surface of the polymer stream; (2) temperature in the mold at 2 mm from the interface; (3) temperature in the mold at 1 mm from the interface; (4): temperature at the surface of the mold calculated using Beck's method.

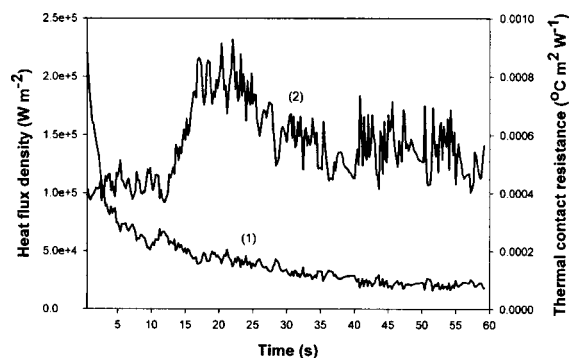


FIG. 6. Surface heat flux (1) calculated using the internal temperatures provided by the two-thermocouple probe, and calculated thermal contact resistance (2).

was disturbed by the air gap appearance and led to a sudden rise of the surface temperature decay signal. This deviation is illustrated by curve 1 in Fig. 5. In addition, the air gap caused the polymer part to cool more slowly, which is exactly observed in the slope change of the temperature history in Fig. 5.

Typical evolutions of temperature in the mold, i.e., temperatures measured with the two-thermocouple probe, are represented by curves 2 and 3 in Fig. 5. Curve 2 refers to the thermocouple located at 2 mm from the mold surface, while curve 3 refers to the thermocouple located at 1 mm from the mold surface. The mold surface temperature resulting from

the inverse calculation is reported in Fig. 5 with curve 4. The surface temperature varied in time and increased by almost 20 °C just after polymer injection. Hence, a constant mold temperature that is usually taken as boundary condition in injection molding software may give rise to inaccurate heat transfer predictions. Furthermore, the heat flux that crossed the polymer-mold interface, also obtained from the inverse calculation, is reported via curve 1 in Fig. 6. This evolution in time is typical of injection molding cycles.<sup>3,4</sup> Heat fluxes are theoretically infinite when the polymer reaches the two-thermocouple probe and then decreases toward zero when the cooling of the part is achieved.

TCR history that resulted from the previously measured and calculated quantities is reported with curve 2 in Fig. 6. The magnitude of TCR was in good agreement with results reported in the literature.<sup>1–3</sup> At short times, TCR did not change as long as high pressure was maintained inside the cavity. When the cavity pressure dropped back to zero, a sudden rise in TCR was observed. The sudden rise of TCR was related to the appearance of the air gap caused by the polymer shrinkage.

<sup>1</sup>A. Bendada, K. Cole, M. Lamontagne, and Y. Simard, *J. Opt. A: Pure Appl. Opt.* **5**, 464 (2003).

<sup>2</sup>J. V. Beck, B. Blackwell, and C. R. St. Clair, *Inverse Heat Conduction* (Wiley, New York, 1985).

<sup>3</sup>Y. Shiraishi, H. Norikane, N. Narazaki, and T. Kikutani, *Int. Polym. Process.* **2**, 166 (2002).

<sup>4</sup>D. Delaunay, P. Le Bot, R. Fulchiron, J. F. Luye, and G. Regnier, *Polym. Eng. Sci.* **40**, 1682 (2000).